Engineered Biocompatible nanoParticles for *in vivo* Imaging Applications

Shu Chen,[a,b] Lijun Wang,[c] Suzanne Duce,[d] Stuart Brown,[c] Stephen Lee,[a] Andreas Melzer,[c] Sir Alfred Cuschieri,[c] Pascal André [a*]
[a] School of Physics and Astronomy (SUPA), University of St Andrews, St Andrews KY16 9SS (UK)
[b] School of Chemistry (EaStChem), University of St Andrews, St Andrews KY16 9ST (UK)
[c] Institute for Medical Science and Technology, University of Dundee, Dundee DD2 1FT (UK)
[d] College of Life Sciences, University of Dundee, Dundee DD1 5EH (UK)

* Pascal.Andre@st-andrews.ac.uk, a.cuschieri@dundee.ac.uk

Supplementary Information

SI-I. Experimental Section

SI-I.1. FePt nPs preparation

Materials: All chemical reagents, unless otherwise stated, were purchased from Sigma, used without further purification but degassed before use: Disodium tetracarbonylferrate-dioxane complex ($Na_2Fe(CO)_4$•1.5 $C_4H_8O_2$), platinum(II) acetylacetonate ($Pt(acac)_2$, 97 %), oleylamine (70 %), oleic acid (90 %), cysteamine (CA, $HSCH_2CH_2NH_2$, BioChemika, ≥ 98.0 %), tetraethylorthosilicate (TEOS, $Si(OC_2H_5)_4$, GC, ≥ 99.0 %), (3-Aminopropyl)triethoxysilane (APTES, $H_2N(CH_2)_3Si(OC_2H_5)_3$, ≥ 98 %), IGEPAL® CO-520 (NP-5, $(C_2H_4O)_n$•$C_{15}H_{24}O$, n ~ 5). When available ACS grade was chosen to select the solvents: dibenzyl ether (≥ 98.0 %), hexane (99.0 %), ethanol (≥ 99.5 %), chloroform (≥ 99 %, anhydrous), methanol (≥ 99.8 %), cyclo-hexane (GC, ≥ 98.0 %), ammonium hydroxide aqueous solution (NH_4OH, 28.0 - 30.0 %).

FePt nPs synthesis: all the syntheses were carried out inside a glove box. A mixture of $Pt(acac)_2$ (1 mmol), oleyl amine (8 mmol) and oleic acid (4 mmol) in 10 mL of dibenzyl ether was placed in a 50 mL round bottom flask connected to a condenser. Under stirring, the mixture was heated up to 100 °C for 1 h to remove oxygen and moisture, then $Na_2Fe(CO)_4$ (1 mmol) in 10 mL dibenzyl ether mixture was added and heated up to 150 °C for 1h. The mixture was further heated up to reflux ~ 300 °C to for 3 h. The dark solution was cooled down to room temperature and after washing with hexane and ethanol, the nPs were collected by centrifugation.[1-2]

fcc-FePt-A: Ligand exchange experiments were carried out in a glove box according to a modified protocol based on the literature.[3] For a typical experiment, 30 mL hexane was added into 3 mL (13.5 mg/mL) of as-synthesized oleic acid/ oleylamine coated fcc-FePt hexane solution. To remove the excess of ligands, the nPs were precipitated by addition of 60 mL ethanol and collected by centrifugation. The nPs were redispersed in 15 mL of chloroform assisted with sonication. 15 mL of cysteamine in methanol solution (0.5 M) was added dropwise to the FePt NPs/$CHCl_3$ mixture under vigorous stirring. The final solution was left under stirring for 48 h to complete the ligand exchange. To extract the nPs, they were redispersed in 10 mL ethanol and sonicated, 20 mL hexane was added and the solution was centrifuged. This process was repeated twice to remove $CHCl_3$, methanol and the excess of ligands. The nPs were then redispersed in 10 mL ethanol and 20 mL deionized water mixture, sonicated and collected by centrifugation. This step was repeated 6 times to obtain positively charged nPs stable in deionized water for more than 8 months (SI-Figure 1).

fcc-FePt-silica-A: The fcc-FePt-silica-A nPs were prepared by hydrolysis of tetraethylorthosilicate (TEOS) and the silica shell surface was further functionalized with (3-aminopropyl) triethoxysilane.[4] Reverse microemulsions were prepared by mixing under vigorous stirring 10 mL cyclohexane, 1.3 mL NP-5 and 50 µL DI H_2O. 2 mg (~ 3-4 nmol) of FePt nPs were then dispersed in 1 mL cyclohexane and added dropwise into the reverse microemulsion. After 15 min, 80 µL TEOS was added dropwise. After another 15 min, 150 µL $NH_4.H_2O$ (28-30 %) was added dropwise. The solution was kept under constant stirring at for 72 h. To form amine functionalized FePt-silica nPs, 100 µL of APTES was added after 48 h and kept stirring for another 24 h. The nPs were precipitated by centrifugation after addition of 3 mL of ethanol and 2 mL of methanol. The nPs were redispersed in 5 mL of ethanol and precipitated by centrifugation after addition of 10 mL of hexane. This step was repeated up to 6 times to completely remove the surfactant. FePt-silica nPs were stable both in ethanol and DI water, while FePt-silica-A nPs were stable in deionized water.

SI-I.2. Experimental Techniques

TEM: Transmission electron microscopy (TEM) images were recorded using a Gatan CCD camera on a JEOL JEM-2011 electron microscope operating at 200 kV. The chemical composition of FePt nPs was examined with energy-dispersive X-ray spectroscopy (EDX) using an Oxford Link system installed in the JEM-2011 microscope.

XRD: Wide-angle powder X-ray diffraction (XRD) data were collected on a Stoe STADI/P powder diffractometer operating in transmission mode and with a small angle position sensitive detector. Incident radiation was generated using a $Fe_{K\alpha1}$ source (λ=1.936 Å). The strongest (111) peak was fitted with Lorentzian-shaped peaks using STOEwinXpow and Kaleida-Graph softwares to precisely determine the diffraction peak positions. The crystalline grain size, D_{XRD}, of the FePt nPs was calculated according to Scherrer's formula:[5]

$$D_{XRD} = \frac{0.9\lambda}{B\cos\theta} \qquad \text{(eq. 1)}$$

where D_{XRD} is the " average" dimension of the crystallites, λ is the wavelength of the X-ray source (for Fe source is equal to 0.193604 nm), B is the full width at half maximum of the peak intensity, θ is the glancing angle.

The atomic composition of FePt NPs was calculated based on the linear relations between lattice constant, a, and Fe percentage, Fe %, reported by Bonakdarkpour et al.[6]

From SI-Figure 1, the following equations can be obtained:

$x_{\%Fe} < 40$ % $a = -0.0014\, x_{\%Fe} + 3.929$ SI-eq. (1)

$x_{\%Fe} > 40$ % $a = -0.0041\, x_{\%Fe} + 4.039$ SI-eq. (2)

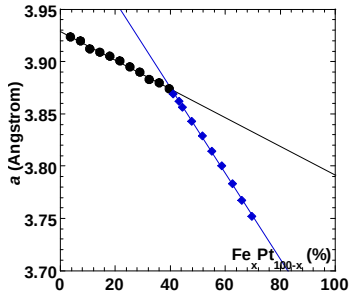

SI-Figure 1. FePt lattice constant (a) analysed by XRD vs. composition curve reported by Bonakdarkpour et al. [6]

SQUID: A 5.0 Tesla Superconducting Quantum Interference Device (SQUID) from Quantum Design (MPMS XL^{TM}) was used to characterize the nPs magnetic properties. The nPs were dispersed in polyvinylpyrrolidone matrix ($V_{Polymer}/V_{nPs}$ = 20) to prevent interaction between the nPs while the resulting sample was loaded into a low background gelatin capsule. Zero-Field Cooled and Field Cooled (ZFC/FC) measurements were completed as follow: the sample was first cooled from room temperature to 2 K without any external field, next a small field 100 Oe was applied and the nPs magnetization was recorded as the temperature was increased up 275 K. The FC curve was obtained by cooling the sample back to 2 K under a 100 Oe magnetic field. The magnetization was then measured while the temperature was increased up to 275 K. Hysteresis measurements were completed at temperatures of 2 K and 300 K. The magnetization of the gelatine capsules and the PVP matrix was subsequently subtracted.

ICP-OES: FePt nPs were dissolved by addition of hydrochloric acid (Trace SELECT®, ≥ 37 %) and nitric acid (Trace SELECT®, ≥ 69.0 %) mixed in 3:1 as volume ratio and left overnight at room temperature. After full dissolution of the nPs, the solution was further diluted with deionised water to prepare inductively coupled plasma-atomic emission spectrometry measurement (ICP-OES, Perkin Elmer Optima 5300 DV).

The conversion of the weight concentration of FePt metal core into Fe molar concentration was completed according to the following equation:

$$[\mathrm{Fe}] = \frac{C_{\text{FePt-A}} R_{\mathrm{Fe}}}{M_{w\text{-Fe}}} \qquad \text{(eq. 2)}$$

where [Fe] (mM) is the molar concentration of iron, C_{FePt} (µg/mL) is the FePt core concentration, $M_{\mathrm{w\text{-}Fe}}$ the molecular weight of the iron atom, R_{Fe} is the mass ratio of Fe in FePt metal core. The mass of the ligand was neglected. The Fe_xPt_{1-x} nPs composition was found to be $x \sim 0.43$ by XRD and ICP-OES. The mass ratio of Fe in the nP core ($R_{\mathrm{Fe}} \sim 0.18$) was calculated with the equation below:

$$R_{\mathrm{Fe}} = \frac{xM_{w\text{-Fe}}}{xM_{w\text{-Fe}} + (1-x)M_{w\text{-Pt}}} \qquad \text{(eq. 3)}$$

A similar approach as described by equation 4 was used for fcc-FePt-silica-A nPs:

$$[\mathrm{Fe}] = \frac{C_{\text{FePt-silica-A}} R'_{\mathrm{Fe}}}{M_{\mathrm{w\text{-}Fe}}} \qquad \text{(eq. 4)}$$

where [Fe] (mM) is the molar concentration of iron, $C_{\mathrm{FePt\text{-}silica\text{-}A}}$ is the concentration of FePt-silica-A in µg/mL, R'_{Fe} is the mass ratio of Fe in FePt-silica-A nPs which is ~ 0.01 according to eq. 5,

$$R'_{\mathrm{Fe}} = yR_{\mathrm{Fe}} \qquad \text{(eq. 5)}$$

where y is the mass ratio of FePt in FePt-silica-A nPs, i.e. $[Fe_xPt_{1-x}]_y[\text{silica-A}]_{1-y}$, which was measured experimentally by ICP-OES and found to be ~ 0.052. As an illustration, according to eq. 4 and 5, the weight concentration of FePt-silica-A nPs at 100 µg/mL corresponds then to ~ 0.02 mM of Fe in molar concentration.

SI-I.3. Cell culture

Materials: Human breast adenocarcinoma cell line MCF7 (ATCC; Cat# HTB-22), human osteosarcoma cell line U2OS (ATCC; Cat# HTB-96) were grown in Dulbecco's Modified Eagle Medium (DMEM; GIBCO, Invitrogen, *Paisley*, *UK*). Human malignant melanoma cell line A375M was kindly provided by Dr Daniele Bergamaschi (*Institute of Cell and Molecular Science*, *Barts and The London*, *Queen Mary's School of Medicine and Dentistry*) and was grown in RPMI-1640 medium (GIBCO, Invitrogen). All media were supplemented with 10 % fetal calf serum, 2 mM glutamine, 100 IU/mL penicillin, and 100 µg/mL streptomycin. Cells were grown under standard cell culture conditions in 5 % CO_2 at 37 °C to reach confluence of 60-70 % before subjected to any further treatments.

Cellular labelling/uptake of FePt nPs and TEM: Cell culture media were removed and replaced with the media containing FePt-A (30 µg/mL). For control experiments, media without FePt-A was used. After 12-16 h of culture, cells were washed and fixed with 4 % (w/v) paraformaldehyde/2.5 % (v/v) glutaraldehyde buffered in 0.2 mol/L PIPES as a standard buffer solution. After 30 min in fixative the cells were scraped off the flasks in1 mL of fixative, transferred to Eppendorf tubes and cetrifuged at 14000 g for 20 min. Pellets were washed in 0.2M PIPES and post fixed in 1 % aqueous osmium tetraoxide for 1 h, washed in water, and dehydrated in graded ethanol and propylene oxide before embedding in Durcupan resin (Sigma) and polymerisation at 60 °C for 24 h. 70 nm sections were cut on a Leica UCT ultramicrotome, mounted on Pioloform coated 100 mesh copper grids, stained with uranyl acetate and lead citrate before being examined in a Tecnai 12 electron microscope. Images were recorded in Digital Imaging Plates and scanned in a Ditabis Micron scanner (Pforzheim, Germany).

Cell viability study by MTS assay: The MTS CellTitre 96 AQueous One Solution Cell Proliferation Assay (Promega, *Southampton*, *UK*) was used to determine cell viability in control and FePt nPs treated cells. This colorimetric assay is based on the conversion of the 3-(4,5-dimethylthiazol-2-yl)-5-(3-carboxy methoxy-phenyl)-2-(4-sulfophenyl)-2H tetrazolium (MTS) compound to a colored, soluble formazan product in metabolically active cells. Cells were seeded at densities 1,250-10,000 cells/well in 96-well plates depending on the duration of incubation time and cultured overnight. Cell culture media were then removed and replaced with the media containing the FePt nPs at various concentrations with the iron content being determined by XRD and ICP-OES. For control experiments, media without FePt nPs was used. MTS assay was performed at specific time intervals by addition of CellTiter 96® AQueous One Solution reagent to each well, in triplicate, and further incubation of cells with the reagent for 3 h at 37 °C in 5 % CO_2. The colour development, i.e. absorbance, was read at 490 nm using a plate-reader (E-Max; Molecular Devices, *CA*, *USA*) and absorbance values of both labelled and control cells were subtracted by that of blank wells. Cell viability in labelled cells was expressed as percentage of that from the corresponding control cells.

Fe release experiment: 3.6 mg (~ 0.6 mg Fe) of FePt fcc-FePt-A nPs in aqueous solution was dispersed in a dialysis tubing (MWCO 1000, Spectrum Laboratories, Inc.) which was further immersed into a 30 mL PBS (pH 4.8) or RPMI-1640 (20 mM

sodium citrate, pH 4.8) bath held at a constant temperature of 37 °C.[7-8] Aliquot buffer solution was then sampled at 6, 12, 24, 48, 72, 168 h, and it composition was subsequently analyzed with ICP-OES.

Prussian blue staining and light microscopy analysis: To gain insight in intracellular iron ions distribution, cells grown on glass coverslips or cytospun on glass slides were washed with PBS to remove the excess of ferumoxides and then fixed with 4 % para-formaldehyde for 30 min. They were then washed with double distilled water (ddH_2O) and incubated for 30 min with 2.5 % potassium ferrocyanide in 2.5 % HCl to produce Fe(III) ferrocyanide (Prussian blue). Samples were then counterstained with nuclear fast red for cell nuclei. Cells were examined using a Zeiss microscope Axiovert 200 (Zeiss, Oberkochen, Germany) at x20, x40 and x63 magnification and Axiovision 4.6 software (Zeiss). Cells were considered Prussian blue positive if intracytoplasmic blue granules could be identified.

Preparation of Agarose Gel Phantoms for MRI of FePt nPs and FePt nP-labeled Cells: In the gel MRI study, 1 % (w/v) low melting point agarose was dissolved in deionized water at 60-70 °C. The desired amount of nPs, i.e. Fe concentration as determined by XRD and ICP-OES was then added to the solution to obtain the targeted concentrations (up to 0.25 mM) and mixed gently. For cellular MRI, FePt labelled melanoma A375M cells were washed three times with PBS and harvested, suspended in low melting point agarose gel (1 % in PBS at densities of 10^4, 10^5, 10^6 cell/mL, respectively. Samples were then transferred into 200 µL thin wall tubes. In both cases, samples were rapidly cooled on ice to form homogenous gel suspensions and kept at 4 °C until further experiments.

Quail Eggs Preparation: Fertilized Japanese quail (Coturnix japonica) eggs were obtained from Rosedean, Huntingdon, Cambs. The eggs were then placed vertically with air sac uppermost in a humidified incubator with a temperature of 38 °C, this was referred to as Day 0. On Day 4, the shell above the air sac was pierced and cut away to remove the inner shell membrane and expose the embryo. The Day 4 embryos typically lay on their sides, the upper eye is visible allowing the solution containing the nPs to be injected into it using syringe with thin glass capillary needle. The top of the eggs were re-sealed with adhesive tape and then imaged. fcc-FePt-A nPs coated with either cysteamine or silica were added to cell culture media at concentrations ranging from 1-100 µg/mL. A control medium without nPs was also used.

SI-I.4. Micro-MRI

Micro-MRI data were acquired on a Bruker Avance FT NMR spectrometer with a wide bore 7.1 Tesla magnet resonating at 300.15 MHz for ^1H, fitted with Bruker micro-imaging magnetic field gradients. A birdcage radio frequency resonator with an internal diameter of 30 mm was used. MRI pulse sequences were taken from the Bruker Paravision® library. All acquisitions were made at 19 ºC. Two acquisition sequences were collected and averaged to improve the signal-to-noise ratio and reduce artefacts.

Relaxation measurements were determined from 128 x 128 axial planes across the samples with field of view of 30 mm, in-plane resolution of 0.234 mm/pixel and image slice thickness of 1 mm. In a typical experiment, 9 tubes were studied simultaneously, gels with no contrast agent acted as a standard. A recycle time (T_R) of 12 s was used to avoid saturation. T_1 relaxation times were measured using an inversion recovery (180º-T_I-90º) imaging pulse sequence; 8 different inversion times (T_I) that ranged from 100 to 15000 ms were applied and the echo time (T_E) was 4 ms.

T_2 relaxation times were measured using a CPMG (Carr Purcell Meiboom Gill) spin echo imaging pulse sequence; a train of 16 echoes was acquired and the delay (τ) between 180º pulses ranged from 8 to 15 ms depending on the samples. Single exponential relaxation times were calculated from experimental data. Each sample was studied three times and average Longitudinal and transverse relaxation rate calculated.

r_i is defined as longitudinal relaxivity (i=1) or transverse relaxivity (i=2), and calculated with the following equation:[9]

$$r_i[CA] = \frac{1}{T_i} - \frac{1}{T_{io}} \qquad \text{(eq. 2)}$$

where [CA] is the concentration of contrast agent, $1/T_i$ (i=1 or 2) is the longitudinal or transverse relaxation rate with the presence of contrast agent, $1/T_{io}$ is the relaxation rate of the medium in the absence of contrast agent.

The 128 x 128 x 128 three-dimensional RARE-8 (rapid acquisition with relaxation enhancement) experiments were acquired with T_R of 250 ms and *TE* between 180º pulses of 25 ms. The field of view was 30 mm and in-plane resolution was 0.234 mm/pixel. The scanning time was 34 minutes.

3D representation of the embryo eye and major blood vessels were produced using Amira® software (Visage Imaging, Inc. San Diego, CA USA).

SI-II. FePt nanoParticles Characterization

SI-II.1. Ligand exchange

Hexane and water are not miscible, and water which is denser (1.0 g/mL vs 0.7 g/mL) lies beneath the hexane phase. This provides a straightforward illustration of the effectiveness of the ligand exchange protocol described in the Section SI-I.1.

The oleic acid and oleylamine capped FePt nPs are only soluble in hexane giving a black color to the upper phase while the DI water remains colorless (SI-Figure 2A). In contrast, SI-Figure 2B presents the cysteamine capped FePt nPs which are soluble in deionized water dispersion leading the lower phase to

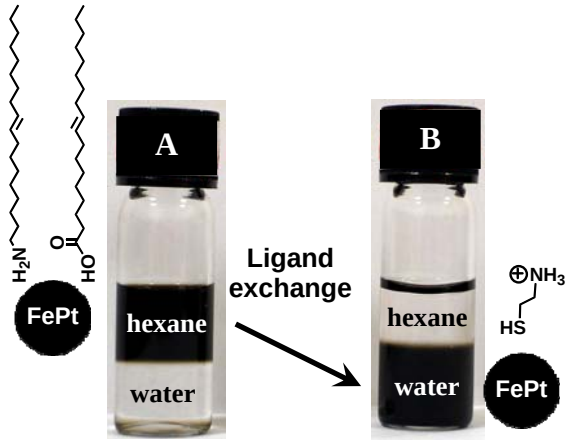

SI-Figure 2. Chemical structure of the ligands and photographs of FePt nPs dispersions in hexane or water phase: oleic acid and oleylamine capped FePt nPs (A), and cysteamine capped FePt (B).

be black whilst the upper hexane phase is remains transparent. After having replaced oleic acid and oleylamine with cysteamine, the nPs are soluble in water solution and stable for more than 8 months.

The efficiency of ligand exchange was then confirmed by Fourier transform infrared spectroscopy (FTIR). The FTIR

spectra of nPs before and after ligand exchange are shown in SI-Figure 3, with all characteristic transmission peaks labelled and matching the literature values.[10] The upper spectra in SI-Figure 3 is characteristic of the nPs coated with oleic acid and oleylamine. The peaks at 1552 and 1713 cm^{-1} can be assigned to the bidendate (-COO-) and monodendate -CO-) modes of oleic acid binding. The shoulder at 1595 cm^{-1} is due to the scissoring mode of the molecularly bonded oleylamine. The two peaks at 2854 and 2924 cm^{-1} correspond to the symmetric and asymmetric -CH_2- stretching modes of the oleyl group. The peak at 3005 cm^{-1} is characteristic of the stretching of =C-H.

The original oleic acid and oleylamine coating of the FePt nPs surface was replaced by cysteamine through the ligand exchange protocol described in Section SI-I.1. It efficiency is demonstrated by the bottom FTIR spectra in SI-Figure 3 characterised by *i*) the

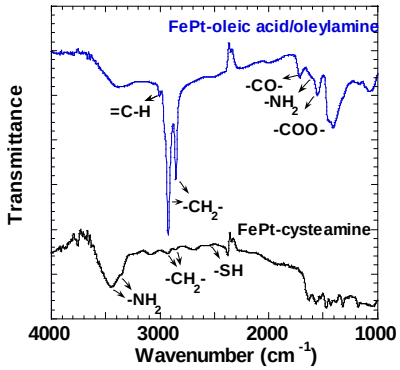

SI-Figure 3. FTIR spectra of as-synthesized nPs coated with oleic acid and oleylamine (top) and cysteamine (bottom) after ligand exchange.

absence of -COO-M and -CO-M, =C-H peaks along with *ii*) the dramatic decrease of the -CH_2- stretching transmission mode. The shoulder at 2560 cm^{-1} is associated with –SH,[11] while the peaks at 3350 and 3448 cm^{-1} are consistent with the –NH_2 end group of the cysteamine.[12]

SI-II.2. Silica Coating

The protocol associated with the silica coating was tuned to provide homogeneous SiO_2 shell as illustrated by the large scale TEM image in SI-Figure 4A. In addition, careful control of the experimental condition prevented the formation of silica nPs without any FePt as illustrated in SI-Figure 4B.

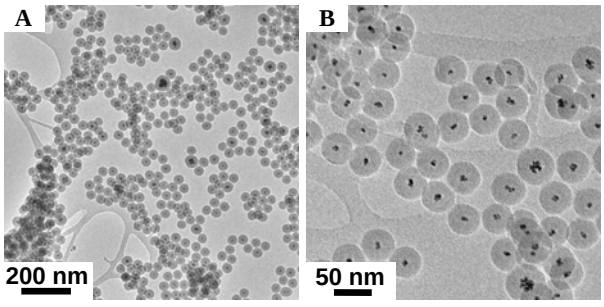

SI-Figure 4. TEM images of FePt coated with a silica shell: low magnification (A), higher magnification (B).

The alteration of the magnetic properties of the nPs after the silica coating (SI-Table 1) is attributed to the formation of thin layers of iron oxide or iron silicide resulting in the reduction of the magnetic effective volume and/or an alteration of the material. In support of this interpretation, the strong base environment associated with the silica coating can partially oxidize the FePt surface resulting in a thin layer of softer magnetic material like iron oxide or iron silicide, which because of its thinness is not visible by XRD or TEM.[13-14]

SI-Table 1. SQUID data of the FePt nPs. T_b is blocking temperature, M_s is the saturation moment and H_c is the magnetic coercivity of the nPs.

Sample	T_b	M_s (2 K)	M_s (300 K)	H_c (2K)
	(K)	*emu per g of Fe*		kOe
fcc-FePt-A	90	201	112	0.7
fcc-FePt-silica-A	50	191	83	1.3

SI-III. Cytotoxicity

SI-Figure 5A and B demonstrate that fcc-FePt-A nPs induce no cell viability damage at concentrations up to 30 µg/mL even after 7 days of incubation. Whilst, the same period of incubation with 60 µg/mL and 120 µg/mL nPs lead to a decrease of the cell viability of only about 80 % and 70 % cell viability, respectively.

The results obtain with MCF7 and U2OS cells are consistent with A375M cells data presented in the core of this publication. As expected the silica layer preserved the cell viability, with SI-Figure 5C showing that fcc-FePt-silica-A nPs did not decrease human cell proliferative activity under culture conditions at concentration up to 200 µg/mL.

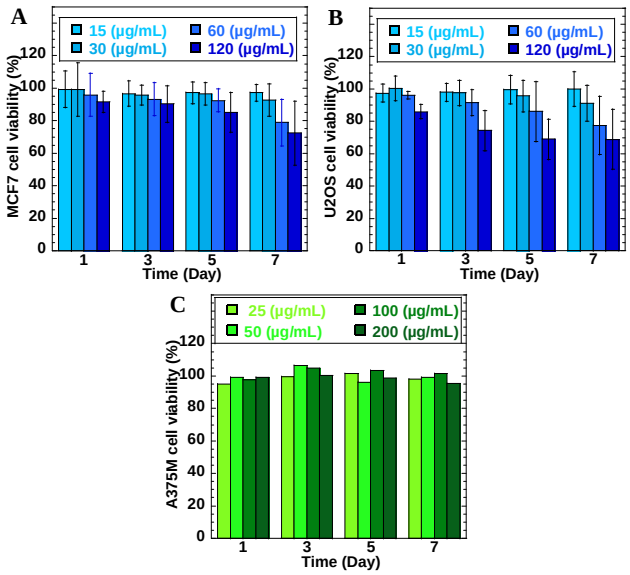

SI-Figure 5. Viability of MCF7 cells (A) and U2OS cells (B) incubated with different fcc-FePt-A nPs concentrations (15, 30, 60, 120 µg/mL), A375M cells (C) incubated with different fcc-FePt-silica-A nPs concentrations (25, 50, 100, 200 µg/mL).

SI-IV. Cellular uptake

SI-Figure 6A illustrates macropinocytosis, one of the main non-specific endocytic pathways which involves the internalization of large areas of plasma membrane together with significant amounts of fluid. Large irregular vesicles called macropinosomes with size larger than 1 µm are generated when membrane protrusions fuse back with the plasma membrane as indicated by the arrows on SI-Figure 6A.

SI-Figure 6B-C present TEM images of A375M cells incubated with fcc-FePt-A nPs at FePt metal core concentration of 30 µg/mL and fcc-FePt-silica-A nPs at nPs concentration of 50 µg/mL after 16 h. SI-Figure 6B shows macropinocytosis uptake mechanism. SI-Figure 6C shows intercellular presence of fcc-FePt-silica-A nPs. Both fcc-FePt-A and fcc-FePt-silica-A nPs demonstrated efficient non-phagocytic human cells internalisation

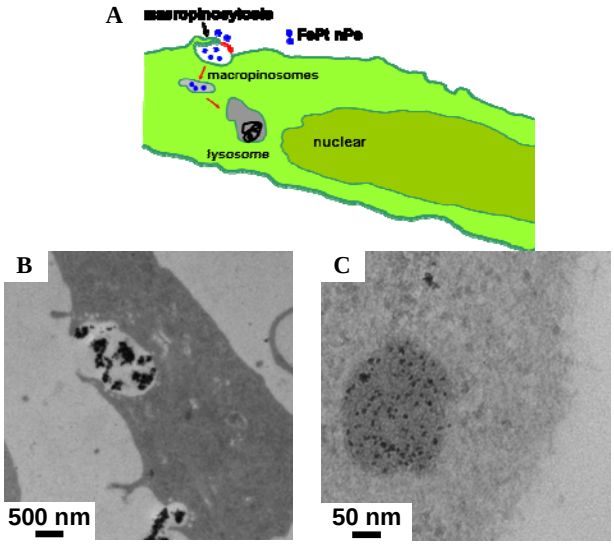

SI-Figure 6. Schematic of cellular uptake through macropinocytosis (A). TEM image of A375M cells after 16 h incubation with DMEM cell media solution containing 30 µg /mL of fcc-FePt-A nPs (B), 50 µg/mL fcc-FePt-silica-A nPs (C).

by straightforward incubation, without any external allied force such as transfection agents or electroporation.

SI-V. MRI

As expected for high magnetic fields such as 7.1 T used in this work,[9] all samples (i.e. Feridex, fcc-FePt-A, fcc-FePt-silica-A) show weak effect on T_1 relaxation time of ^{1}H in 1 % agarose gel water solution (SI-Figure 7A).

SI-Table 2 summarizes the relaxivity values r_1 and r_2 obtained in this work and compare them with iron oxide data previously published. The relaxivities values obtained with Feridex are consistent with literature's values. In addition and as presented in the core of the publication, it is noticeable that higher r_2 values were obtained with fcc-FePt based nPs compared with Feridex'.

SI-Table 2. ^{1}H relaxivity values (r_1 and r_2) for agarose gel solution containing Feridex I.V.®, fcc-FePt-A and fcc-FePt-silica-A nPs compared to values of some commercial contrast agent base on literature (7.1 T, 300 MHz MRI, 37 ºC, in water).[9]

Sample	r_1 ($s^{-1}mM^{-1}$)	r_2 ($s^{-1}mM^{-1}$)
fcc-FePt-A	2.5 ± 1.0	887 ± 32
fcc-FePt-silica-A	0.3 ± 0.1	210 ± 3
Feridex I.V.® (Ferumoxides)	0.9 ± 0.1	148 ± 2
Feridex I.V.® as reported	1.8*	132*
Ferucarbotran. A®	1.6*	205*
Ferumoxtran-10®	1.4*	71*
Ferumoxytol®	2*	95*

*Experimental uncertainty was not reported.

SI-Figure 7B shows that at a magnetic field of 5 T and a temperature of 300 K, fcc-FePt-A nPs have the highest magnetization of 112 emu/g of Fe; however, fcc-FePt-silica-A nPs and Feridex appear to have similar nPs magnetizations of about 80 emu/g of Fe. By design, the commercial SQUID magnetometer highest external magnetic field is 5 T, whilst MRI experiments were performed at 7.1 T. However, a higher nPs magnetization of fcc-FePt-silica-A nPs compared to Feridex can be expected by extrapolating the magnetization curves on SI-Figure 7 from 5 T to 7.1 T. It is indeed noticeable that Feridex has already saturated at 5 T, while the silica coated FePt nPs had yet to reach saturation magnetization.

SI-Figure 8 illustrates the effect of injecting embryo with fcc-FePt-A nPs (1 mg/mL, SI-Figure 8, top row) and fcc-FePt-silica-A nPs (27 µg/mL FePt core concentration, i.e. 560 µg/mL FePt-

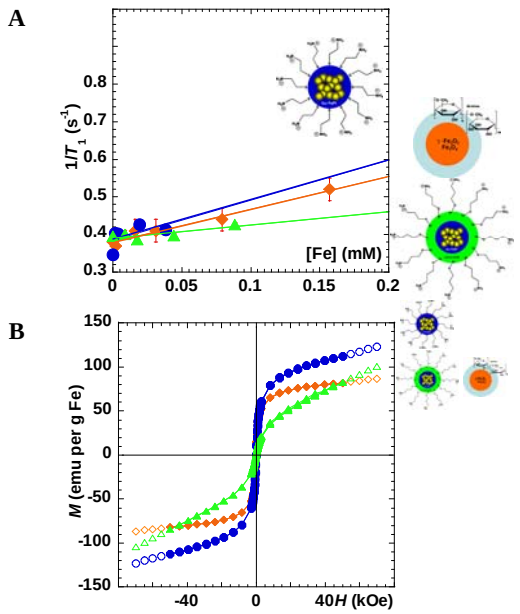

SI-Figure 7. T_1^{-1} (s^{-1}) vs. [Fe] (mM) curve which illustrates 7.1 T MRI studies of the effect of the presence of (blue ●) fcc-FePt-A, (green ▲) fcc-FePt-silica-A and (orange ♦) Feridex I.V.® samples on ^{1}H longitudinal (T_1) relaxation time of the water in 1 % w/v agarose gel (A). Hysteresis curves of fcc-FePt-A nPs (blue ●), fcc-FePt-silica-A nPs (green ▲) and Feridex (orange ♦) at 300 K. The empty symbols are magnetisation values extrapolated at 7 T (B).

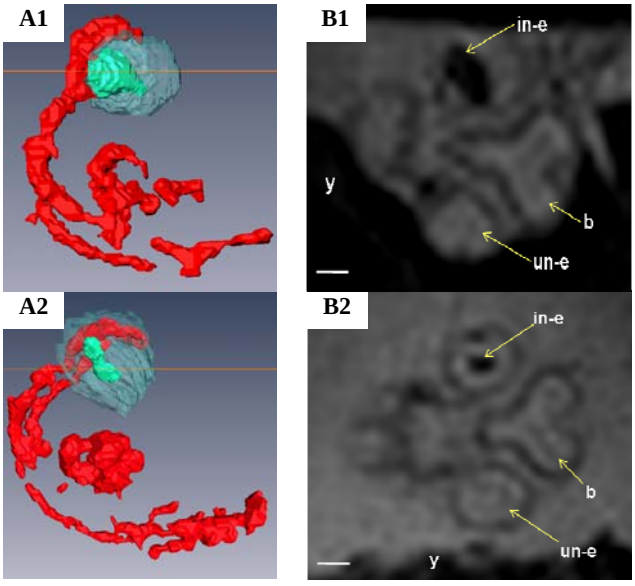

SI-Figure 8. Embryo injected *in ovo* with cell culture media (1 µL) containing 1 mg/mL fcc-FePt-A nPs (top row) and fcc-FePt-silica-A nPs at FePt core concentration 27 µg/mL (bottom row). 3D surface reconstruction of embryo eyes (blue) and blood vessels (red) showing the position in yellow of the transverse images (A); Dorsal view of transverse image of the embryo's head aligned through the eyes (B). 2D slices from 128x128x128 3D Rare-8 MRI data set of Day 4 quail embryo egg (T_R / T_E = 250 / 25 ms), field of view of 30 mm and pixel dimensions of 0.234mm/pixel. Label: y = yolk, b = brain, in-e = injected eye, un-e = un-injected eye; scale bar indicates 1mm.

silica-A concentration, SI-Figure 8, bottom row). SI-Figure 8A are 3D surface reconstruction which have been processed to highlight embryo eyes in blue, the blood vessels in red, and the nPs in green. In both cases, the presence of the nPs solution produced a strong hypointensity in the images clearly visible because of the darker contrast when comparing with the eye which has not been injected (SI-Figure 8B).

References

(1) Chen, M.; Liu, J. P.; Sun, S. *J Am Chem Soc*. **2004,** 126, 8394-8395.
(2) Nguyen, H. L.; Howard, L. E. M.; Stinton, G. W.; Giblin, S. R.; Tanner, B. K.; Terry, I.; Hughes, A. K.; Ross, I. M.; Serres, A.; Evans, J. S. O. *Chem Mater*. **2006,** 18, 6414-6424.
(3) Tanaka, Y.; Maenosono, S. *J Magn Magn Mater*. **2008,** 320, L121-L124.
(4) Koole, R.; van Schooneveld, M. M.; Hilhorst, J.; Donega, C. D.; 't Hart, D. C.; van Blaaderen, A.; Vanmaekelbergh, D.; Meijerink, A. *Chem Mater*. **2008,** 20, 2503-2512.
(5) Azaroff, L. V., *Elements of X-ray Crystallgraphy*. 1st ed.; McGraw-Hill, Inc.: New York, 1968.
(6) Bonakdarpour, A.; Wenzel, J.; Stevens, D. A.; Sheng, S.; Monchesky, T. L.; Lo¨bel, R.; Atanasoski, R. T.; Schmoeckel, A. K.; Vernstrom, G. D.; Debe, M. K.; Dahna, J. R. *J. Electrochem. Soc.* **2005,** 152, A61-72.
(7) Xu, C. J.; Yuan, Z. L.; Kohler, N.; Kim, J. M.; Chung, M. A.; Sun, S. H. *J Am Chem Soc*. **2009,** 131, 15346-15351.
(8) Arbab, A. S.; Wilson, L. B.; Ashari, P.; Jordan, E. K.; Lewis, B. K.; Frank, J. A. *Nmr Biomed*. **2005,** 18, 383-389.
(9) Modo, M. M. J.; Bulte, J. W. M., *Molecular and Cellular MR Imaging*. 1st ed.; CRC Press: London, 2007.
(10) Bagaria, H. G.; Ada, E. T.; Shamsuzzoha, M.; Nikles, D. E.; Johnson, D. T. *Langmuir*. **2006,** 22, 7732-7737.
(11) Torimoto, T.; Tsumura, N.; Nakamura, H.; Kuwabata, S.; Sakata, T.; Mori, H.; Yoneyama, H. *Electrochim Acta*. **2000,** 45, 3269-3276.
(12) Koji, N., *Infrared Absorption Spectroscopy*. 1 st ed.; Holden-Day, Inc., San Francisco and Nankodo Company Limited, Tokyo: 1962.
(13) Lee, D. C.; Mikulec, F. V.; Pelaez, J. M.; Koo, B.; Korgel, B. A. *J Phys Chem B*. **2006,** 110, 11160-11166.
(14) Thomson, T.; Terris, B. D.; Toney, M. F.; Raoux, S.; Baglin, J. E. E.; Lee, S. L.; Sun, S. *J. Appl. Phys.* **2004,** 95, 6738-6740.